Advances in Science and Technology Research Journal, 2025, 19(12), 100–108 https://doi.org/10.12913/22998624/209741 ISSN 2299-8624, License CC-BY 4.0

Published: 2025.11.01

Received: 2025.05.09

Accepted: 2025.10.01

Study of agglomerated TiO₂ and TiO₂+Cr₂O₃ nanocoatings deposited by air plasma spraying on erosion wear

Baurzhan Rakhadilov¹, Garip Erdogan¹, Zhangabay Turar¹,2*, Dauir Kakimzhanov¹

- ¹ PlasmaScience LLP, Ust-Kamenogorsk 070000, Kazakhstan
- ² Sakarya University, Thermal Spray Research and Application Laboratory, Sakarya 54050, Turkey
- * Corresponding author's e-mail: turarjanabay@gmail.com

ABSTRACT

In this study, agglomerated TiO₂ and TiO₂ nanopowders with Cr₂O₃ addition were tested for erosive wear in a slurry environment. Their abrasiveness, mass loss, and volume loss were investigated. The slag slurry was sieved to an average particle size of 450–515 μm, and media containing 10 wt% slag were prepared. Experiments were conducted at particle velocities of 2 m/s and 4 m/s with normal impact angles (90°). The results revealed that TiO₂+Cr₂O₃ nanocoatings exhibited approximately 25% higher resistance to erosive wear compared to pure TiO₂ coatings. Moreover, wear increased with rotational speed, highlighting the influence of mechanical conditions on coating performance. Overall, the addition of Cr₂O₃ significantly enhanced the mechanical stability and durability of the coatings. These findings provide important insights into the wear mechanisms of nanopowder-based coatings and demonstrate the potential of TiO₂+Cr₂O₃ systems for improving the performance and service life of components operating under high-wear conditions, particularly in industries involving abrasive slurry flows and particulate impact, such as mining, energy, and chemical processing.

Keywords: coatings, plasma spraying, agglomeration, structure, erosion wear.

INTRODUCTION

Erosive wear is one of the main challenges in various industrial sectors where components are exposed to high-velocity slurry or particulate flows. Systems such as pipelines, pumps, turbines, and valves [1, 2] often suffer from mechanical degradation due to continuous particle impacts, leading to significant maintenance costs and reduced operational efficiency. Enhancing the wear resistance of exposed surfaces is therefore a crucial technological goal, particularly through advanced protective coatings.

In recent years, plasma-sprayed ceramic coatings have gained attention for their ability to form hard, wear-resistant layers [3–5]. Among these, titanium dioxide (TiO₂) and its composites are widely studied due to their favorable mechanical properties and chemical stability. The incorporation of secondary oxides such as chromium oxide (Cr₂O₃) into TiO₂ matrices [6, 7] has been

proposed to further improve hardness, erosion resistance, and coating adhesion.

Building on this context, prior studies have examined the mechanisms of erosive wear in both ductile and brittle materials. Finnie [8] first examined erosive wear, which means the breakage of particles in a fluid medium as a result of their contact with any surface during their movement with the fluid, in detail as solid particle wear. In another study, he discussed erosive wear on ductile materials [9]. Bitter [10], on the other hand, defined wear in solid transport in liquid media in two different types as simultaneously acting deformation and shear wear, and formulated the wear phenomenon according to the mechanical and physical properties of the abrasive and the abraded material. In another study, he explained many erosive wear phenomena with formulas and presented findings for the prevention and reduction of erosive wear in practice [11]. Shipway and Hutchings [12] defined erosive wear as the removal of material from a surface by the impact of abrasive particles and stated that the rate of erosive wear depends on both the target material and abrasive properties and the impact conditions of the abrasive. Lindsley and Marder [13] concluded that particle velocity is a critical experimental parameter in erosive abrasion; the effects of different velocities on the target material can be easily distinguished, and an increase in erosive abrasion is obtained by increasing the velocity. Barton [14] stated that solid particles such as sand hitting the inner surface of the pipe, valves, fittings and other components of the system cause mechanical wear as well as possible system damage, and that erosive wear is the primary factor that shortens the material life of equipment used in industry, especially in fluid environments where solid particles are transported. Regarding the conditions, the type of fluid medium, the shape [15], size [16], concentration in the fluid, impact angle [17], impact velocity [18], and temperature of the fluid medium are considered effective parameters [19], while parameters such as toughness and hardness are important for the worn material [20]. Many studies have been conducted to investigate the effects of these parameters on both ductile [21] and brittle materials. In order to carry out these studies, many experimental methods and experimental setups have been developed for the application of these methods [22]. For example, Desale et al. [23] designed a setup in which the experiments were carried out in a chamber, and design measures were taken to minimize the random movement of abrasive particles. They conducted studies in which a stirrer (with a downward motion of the mixture) was used to minimize the relative velocity between the sample and the abrasive particles. Moreover, they created different conditions to measure the effects of abrasive impact angle, concentration, velocity, and particle size parameters on erosive wear. This chamber experimental setup is aimed at predicting erosion of equipment such as pipes, elbows, and pumps at reasonable concentration ratios and actual flow rates, and to obtain more realistic results. In this study, agglomerated TiO2 and Cr2O3 nanopowders coated with TiO2 and TiO2+Cr2O3 coated by air-plasma spraying were used to study the erosion induced by slag attack on the coatings. The study was carried out at varying particle velocities, the results were compared, and the wear was evaluated by mass and volume loss. SEM images were also taken before and after the study.

EXPERIMENTAL STUDIES

Preparation of abrasive particles and slurry

The percentage distribution of slag particle sizes to be used as abrasive was obtained, and it was found that approximately 65% of the slag had a size ranging from 300 µm to 800 µm. The slag was sieved to remove very fine and very large particles, after which the average size of the abrasive particles was approximately 515 µm.

For each speed condition (2 m/s and 4 m/s), two types of coatings were tested: TiO_2 and $TiO_2+Cr_2O_3$. For each type of coating in each condition, two samples (n = 2) were prepared and analyzed to ensure the statistical reliability of the measurements of hardness, roughness, and wear.

The SEM image of the slag, whose chemical composition was obtained by the TESCAN VEGA device at 15 kV, is given in Table 1 and shown in Figure 1 before and after the screening process. As seen from the SEM image, the abrasive particles are irregularly shaped metal particles. Surface roughness (Ra) was measured using a Mitutoyo Surftest profilometer, averaging multiple points per sample. The friction coefficient was determined by a pin-on-disc tribometer under controlled load and sliding speed conditions.

Figure 1 shows the SEM image of the slag, whose chemical composition was obtained by the TESCAN VEGA device. Table 1 shows the slag before and after the screening process.

Specimens

Within the scope of this study, experimental specimens: TiO_2 nanopowder coated on a titanium substrate and $TiO_2+Cr_2O_3$ nanopowder coated using the APS method with 190 μ m and 250 μ m thickness (Figure 2) were used. The samples' weight and surface roughness values were measured before the slurry erosion experiment. Figure 3 shows SEM images of the sample surfaces before the experiment.

Slurry erosion experiments

Before the experiment, the samples were cleaned and weighed on a scale to the nearest 0.0001 mg. The same cleaning process was repeated after the experiments. After the samples were placed in the holder, they were fixed using the fixing bolts. The duration of the experiments

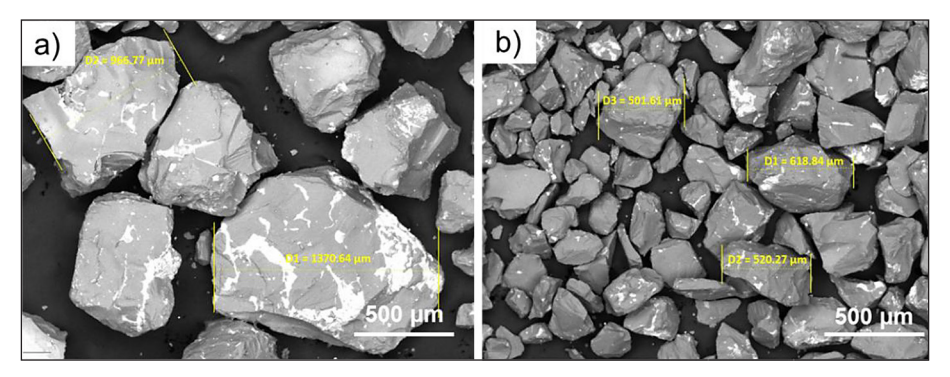


Figure 1. SEM images of granulated blast furnace slag: (a) before sieving; (b) after sieving

Table 1. The chemical composition of the granulated blast furnace slag sample [wt%]

		0	Al	С	Ti	Pb	Bi	F	Se	Si	Other
ĺ	[wt%]	46.86	40.12	6.01	1.59	0.96	0.62	0.48	0.38	0.41	2.57

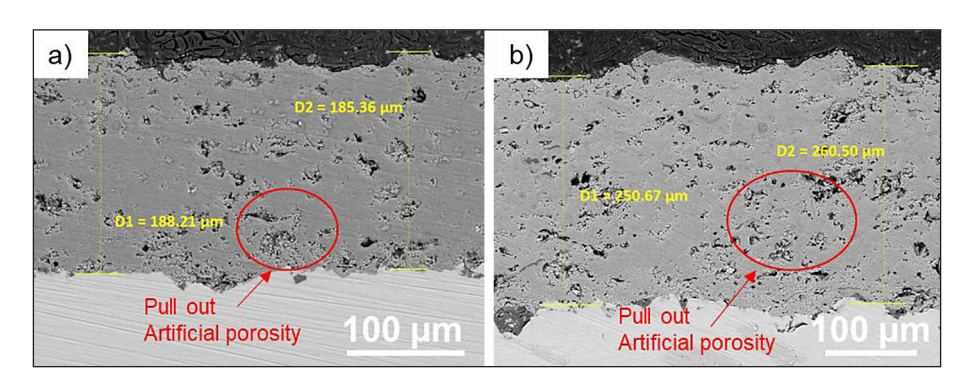


Figure 2. Cross-section of coverings with cover dimensions: (a) TiO₂; (b) TiO₂+Cr₂O₃

was limited to 30 minutes so as not to reduce the particle size on the abrasive surfaces.

After the end of the first experiment, the old slag was removed from the system, and the new slag prepared beforehand was added to the system. After the experiments, it was determined that approximately 60% of the slag remained within the same range of values in terms of particle size,

and the rest of the slag fell below 300 μ m [24]. Again, after the experiment, the inner surfaces of the sample holders were cleaned with pressurized water to prevent the formation of residue inside the sample holders.

Figure 3 shows the surface morphology of the samples before the wear tests: (a) pure TiO_2 coating, exhibiting a relatively smooth

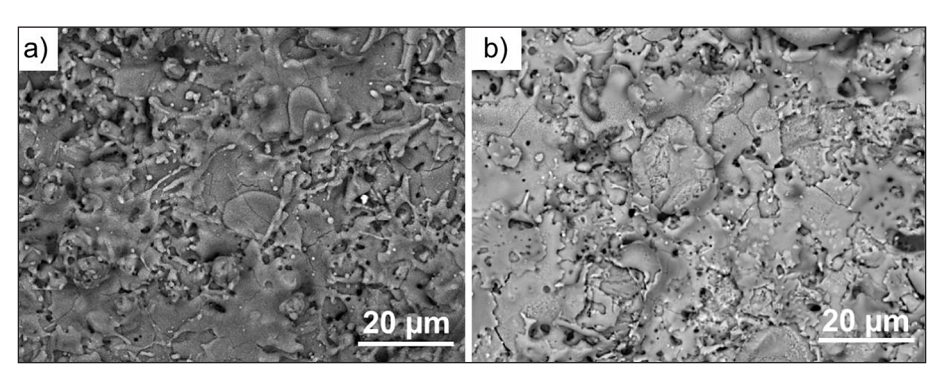


Figure 3. (a) TiO₂ coating; (b) TiO₂+Cr₂O₃ coating

	<u> </u>				
Sample	TiO ₂	TiO ₂ +Cr ₂ O ₃	TiO ₂	TiO ₂ +Cr ₂ O ₃	
Speed (m/s)	2	2	4	4	
Hardness Value [HV-100 kgf]	700 ± 31	964 ± 42	700 ± 31	964 ± 42	
Ra [µm]	4.726	5.633	4.793	5.693	
Sample front weight [kg]	8.7891	9.1378	9.5462	9.6358	

Table 2. Surface hardness, weight, and roughness values of the samples

and uniform surface; (b) TiO₂+Cr₂O₃ composite coating, demonstrating a rougher texture due to the presence of chromium oxide particles.

The slurry was prepared at 2 different velocity values in the present study to investigate these parameters. The 260 rpm and 520 rpm speeds correspond to 2 m/s and 4 m/s, respectively. The stirrer impeller used to prevent the slag from settling to the bottom of the hopper also ensured that the mixture had a uniform structure. In addition, the propeller blade positions were designed so that the slag movements were designed to move from the center towards the chamber wall and then upwards. During the experiment, four plates on the chamber walls prevented the slag particles from making circular movements in the

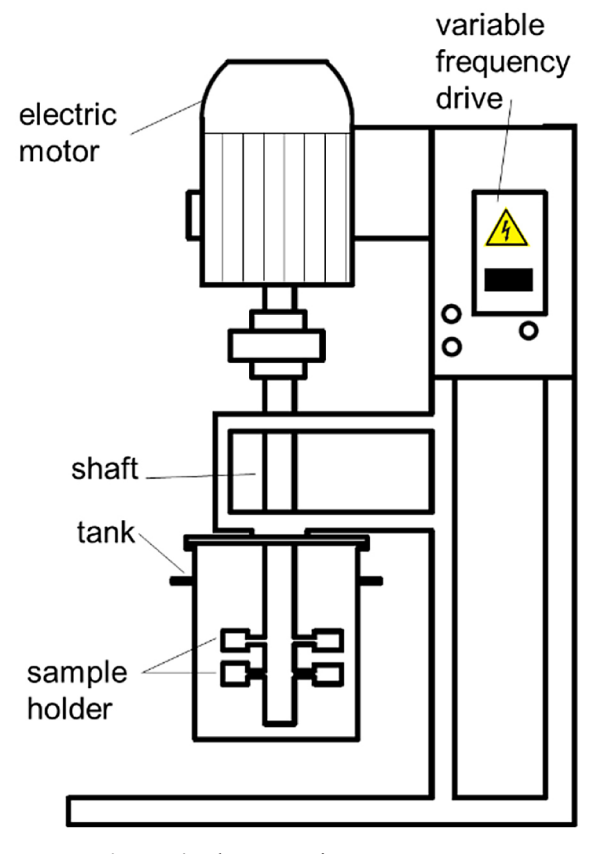


Figure 4. Slurry erosion test apparatus

direction of sample rotation. In addition to the speed, the solid concentration was selected at a different value, 10%. The specimen clamping angles were not changed, and the experiments were carried out only at the normal impact angle. In the section devoted to the assessment of coating wear resistance, the experimental parameters presented in Table 3 were used, as well as the measurement results presented in Table 2.

RESULTS AND DISCUSSIONS

Figure 5 shows the XRD analysis results of TiO₂ and TiO₂ + Cr₂O₃ nanocoatings. It is known that titanium and oxygen have many different compounds (TiO, TiO2, Ti3O, Ti3O2, etc.), and Ti₂O is one of these phases. The properties of titanium phases depend on the production method and composition. By studying the phase diagram of Ti-O, it can be seen that the TiO₂ phase is formed under conditions containing more than 60% oxygen 1 [25]. The XRD pattern of the TiO₂ coating layer showed that the coating consisted mainly of the rutile (R-TiO₂) phase with a small amount of the anatase (A-TiO₂) phase. In the plasma spraying process, since most of the TiO2 powder was melted and atomized onto the surface, it is extremely difficult to preserve the structure of the metastable anatase phase. In a study conducted by Yang et al [26], it was observed that regardless of the crystal structure of the powder fed, most of the TiO2 coatings obtained by plasma spraying consisted of a rutile phase and contained very little anatase in their structure. In addition, the ZrO₂ phase, which was present in small amounts in our TiO2+Cr2O3 coating, originated from the zirconia lining of the attritor during milling. Since no ZrO2 phases were detected in the TiO2 coating, it can be concluded that the addition of Cr2O3 led to slight wear of the zirconia lining of the attritor.

Table 3. Experimental setup parameters

Sample	TiO ₂	TiO ₂ +Cr ₂ O ₃	TiO ₂	TiO ₂ +Cr ₂ O ₃
Speed (m/s)	2	2	4	4
Concentration (wt.%)	10%	10%	10%	10%
Angle (°)	90	90	90	90
t (min)	30	30	30	30

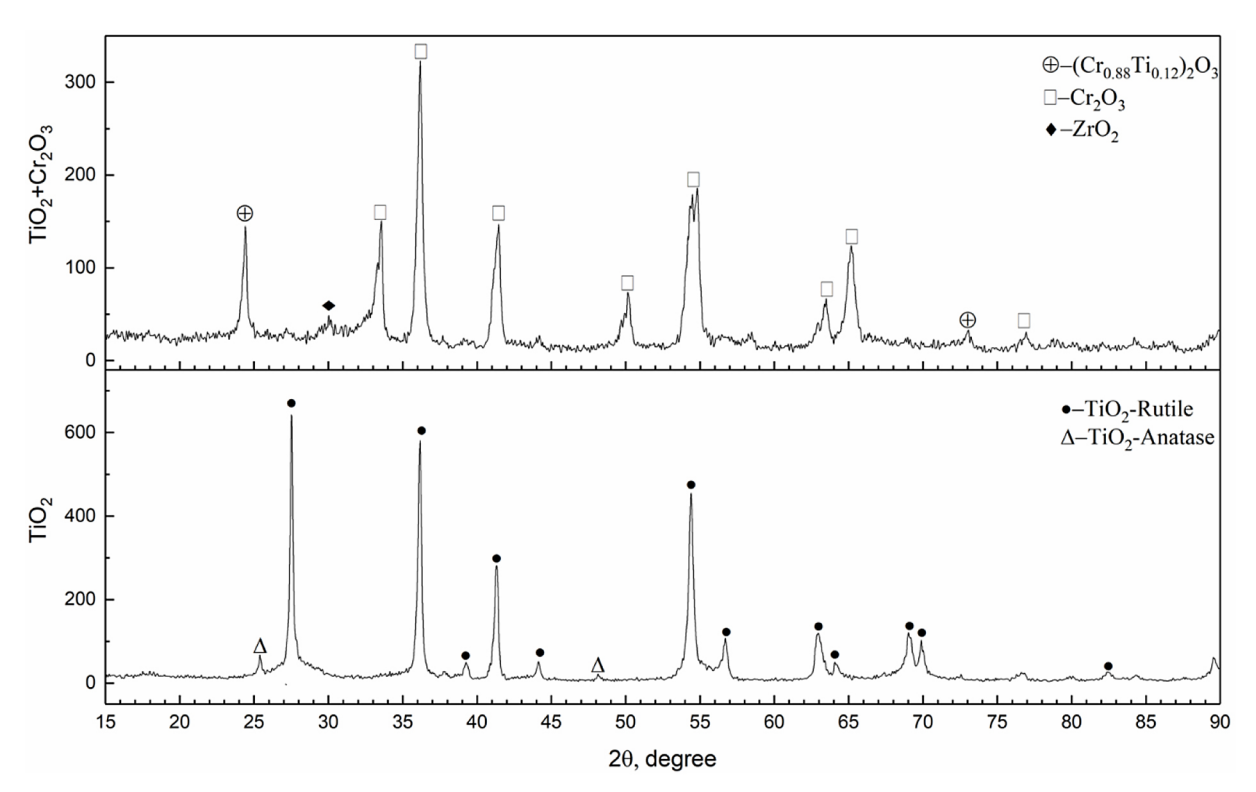


Figure 5. XRD spectra analyses

Wear quantity

The graphs show the dependence of the friction coefficient μ on the path L for TiO₂ (a) and TiO₂+Cr₂O₃ (b) coatings with an aluminum ball as a counterbody. In both cases, a sharp increase in μ at the beginning and then its stabilization is observed. The sharp increase in μ is due to the run-in phase: coating roughnesses are smoothed, surfaces are adapted, and wear particles can be released. After the formation of a stable contact zone, the coefficient of friction stabilizes. The Ti-O₂+Cr₂O₃ coating shows a slightly higher but stable coefficient of friction [5, 27] (~0.9) compared to TiO₂ (~0.8–0.9). This indicates increased wear resistance and improved mechanical stability of the composite coating.

As a result of the experiments carried out at different speeds, weight losses were measured in order to make an accurate comparison due to the different values of the core weights of the samples. The weight losses of the coatings as a result of these measurements are summarized in Table 4: TiO₂ (0.0131 mg) and TiO₂+Cr₂O₃ (0.0099 mg) at 2 m/s; TiO₂ (0.1131 mg) and TiO₂+Cr₂O₃ (0.912 mg) at 4 m/s. In light of these data, it can be concluded that TiO2+Cr2O3 coatings exhibit resistance to erosive wear. As shown in Table 4, the material loss increased linearly with increasing speed. In addition, TiO2+Cr2O3 coatings exhibited the lowest material loss at both speeds [6, 27]. This is because Cr₂O₃ has high hardness, which improves the mechanical strength of the coating. The harder material is less susceptible to mechanical failure when exposed to abrasive particles, which reduces the wear rate.

As seen in Figures 7 and 8, the average roughness values of the worn surface are presented. The higher surface roughness loss of the

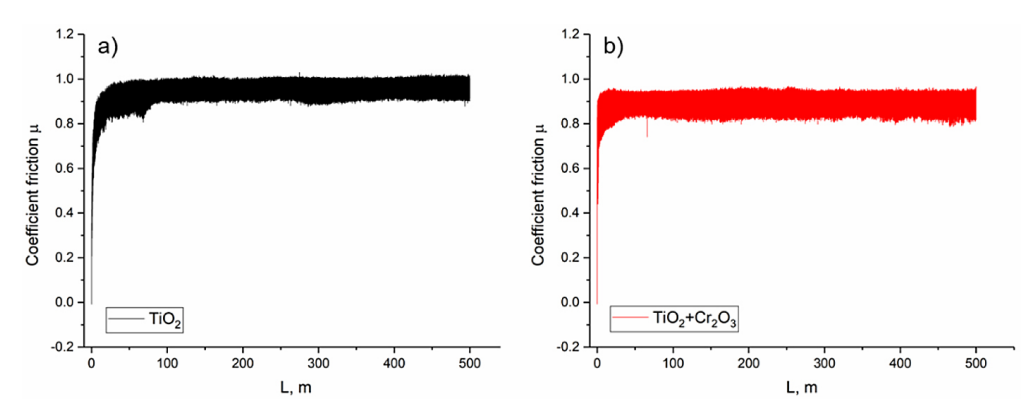


Figure 6. Dependence of the friction coefficient of coatings on the length of the friction path

Table 4. Weight and surface roughness values of the specimens after the test

Sample	TiO ₂	TiO ₂ +Cr ₂ O ₃	TiO ₂	TiO ₂ +Cr ₂ O ₃	
	2 m/s	2 m/s	4 m/s	4 m/s	
Weight [kg]	8.7760	9.1279	9.4331	9.5446	
Ra [µm]	2.690	3.839	2.903	2.189	

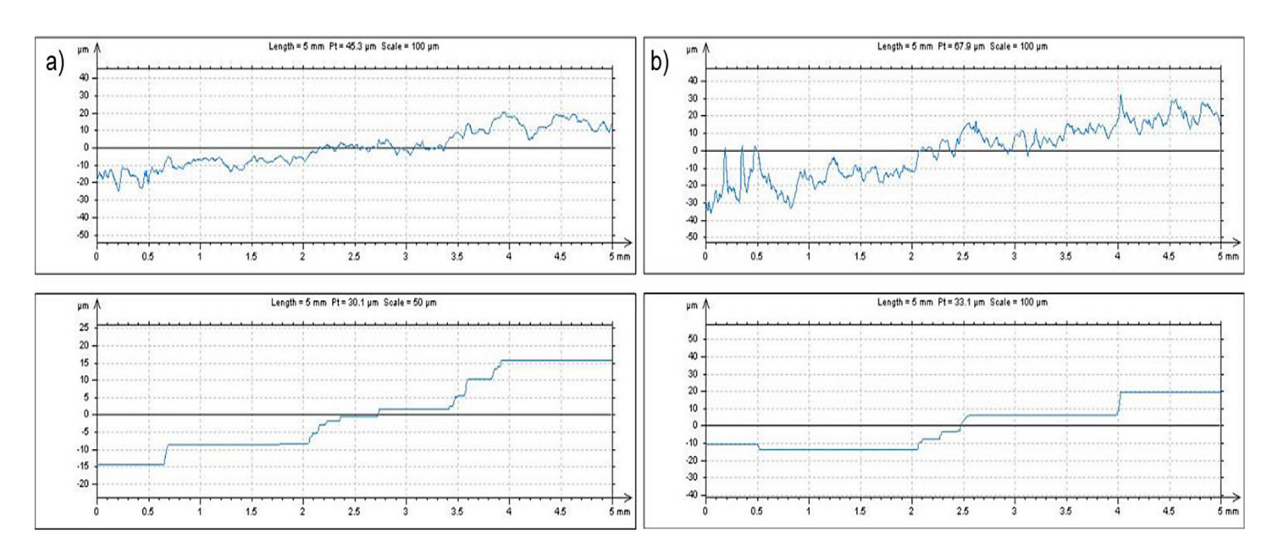


Figure 7. Surface roughness value and volume loss at 2 m/s speed: (a) TiO₂ coating; (b) TiO₂+Cr₂O₃ coating

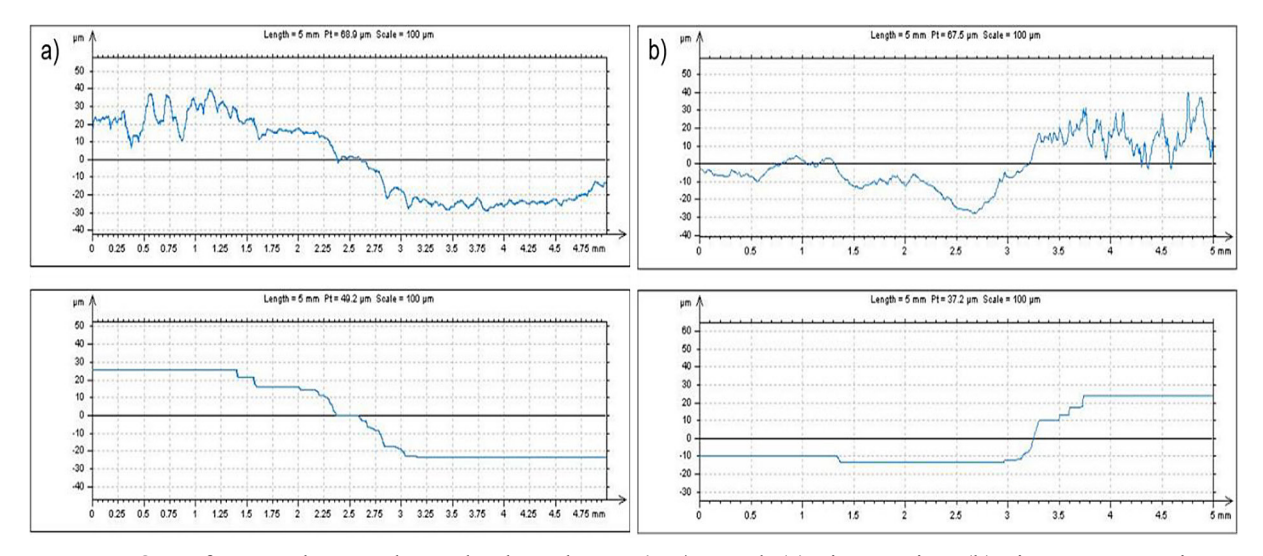


Figure 8. Surface roughness value and volume loss at 4 m/s speed: (a) TiO₂ coating; (b) TiO₂+Cr₂O₃ coating

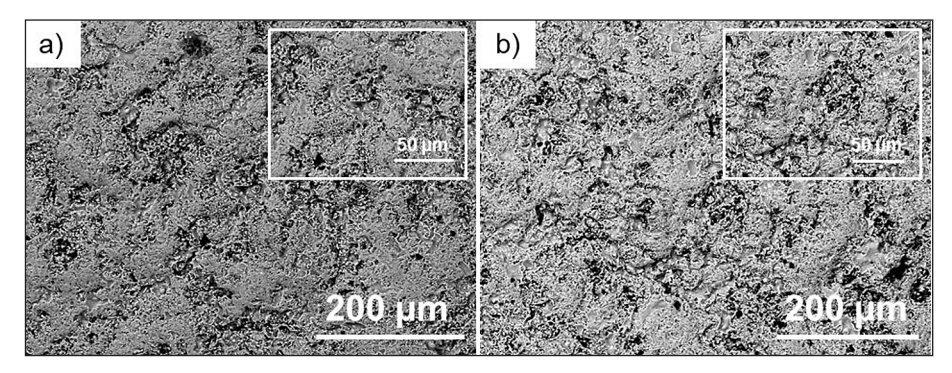


Figure 9. Surface images at 2 m/s velocity: (a) TiO₂ coating; (b) TiO₂+Cr₂O₃ coating

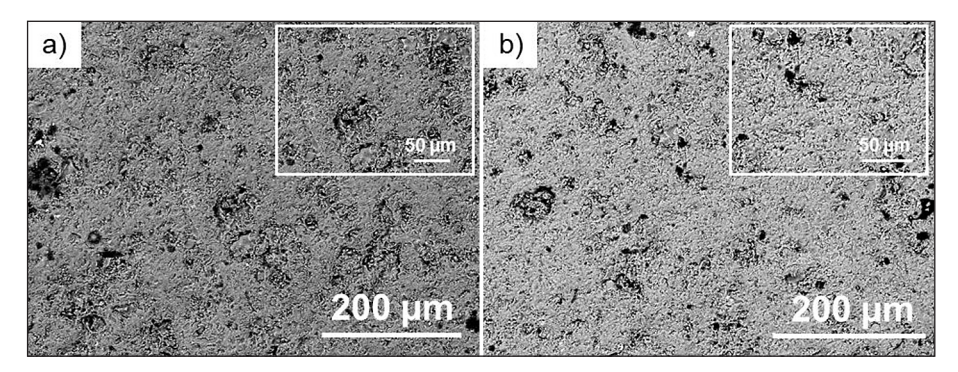


Figure 10. Surface images at 4 m/s velocity: (a) TiO₂ coating; (b) TiO₂+Cr₂O₃ coating

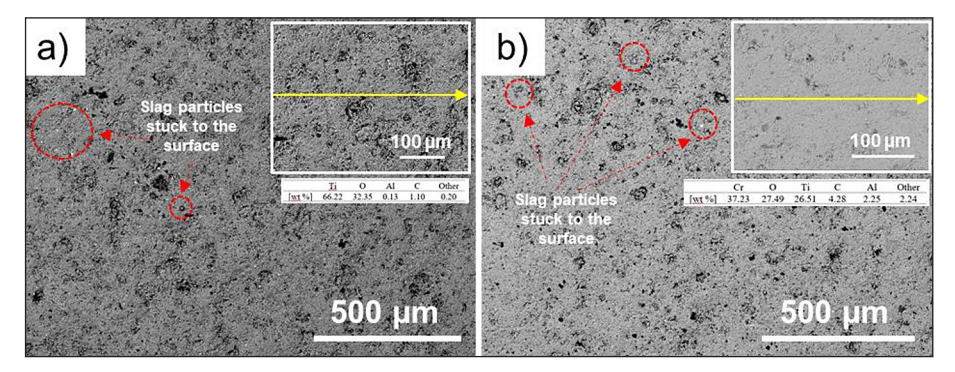


Figure 11. Surface images at 4 m/s velocity and chemical composition of the samples [wt%]: (a) TiO₂ coating; (b) TiO₂+Cr₂O₃ coating

TiO₂-coated sample compared to the TiO₂+Cr₂O₃ coating is explained by the difference in the wear degree of the regions.

Wear surfaces

SEM images of the sample top surfaces were obtained as a result of the experiments performed at 2 m/s for TiO₂ and TiO₂+Cr₂O₃ samples in Figure 9 and at 4 m/s in Figure 9. At an impact angle perpendicular to the surface (90°), plastic deformation is the dominant wear mechanism of the specimen surfaces, so deep damage zones occur. Limited shear abrasion marks, which usually

occur in angular particle impacts, are very rare [23, 24]. As can be seen from the images, the surface of the specimen is smoothed, and the roughness slightly decreases. With the increase in velocity, the coating smoothing caused by abrasion is observed on the material surface. The images in Figures 7 and 8 for TiO₂ and TiO₂+Cr₂O₃ coatings clearly demonstrate this trend.

As can be seen in Figure 10, the surface of samples at 4 m/s with TiO₂ and TiO₂+Cr₂O₃ coating does not have a homogeneous structure as at 2 m/s. Particle inclusions are observed at different locations. The results of the percentage distribution of elements belonging to the

linear distribution are summarized in Figure 11. As can be seen, the colored areas indicated by red lines are areas of particle embedding in the coating surface.

CONCLUSIONS

Based on the research conducted, the following conclusions can be drawn:

- 1. XRD analysis showed that the TiO₂ coating consists predominantly of the rutile phase with negligible anatase content, which is due to the thermal stability of the rutile modification during plasma spraying. The introduction of Cr₂O₃ not only contributed to the preservation of the rutile structure but also led to the appearance of traces of ZrO₂, which indicates slight wear of the zirconium lining of the attritor during the mechanical grinding process.
- 2. This study demonstrates improved wear resistance and mechanical stability of TiO₂+Cr₂O₃ composite coatings, as evidenced by the higher but stable coefficient of friction observed in tribological tests. The initial increase in friction in the "entry" phase, followed by its stabilization, reflects the typical adaptation of the surfaces during sliding. The advantage of the TiO₂+Cr₂O₃ coating over pure TiO₂ highlights the potential of chromium oxide addition to improve the durability and functionality of thermally sprayed coatings. The results contribute to the understanding of wear mechanisms in nanopowder-based coatings and open avenues for further optimization in applications where high wear resistance is critical.
- 3. Based on the results of the erosion wear test, it can be concluded that with increasing speed (from 2 m/s to 4 m/s), there is a significant deterioration of the coating structure. At 4 m/s, the mass loss of the coating becomes more pronounced and the structure becomes less homogeneous, with the formation of particle inclusions at different points. This is also confirmed by the results of the percentage distribution of elements over the linear distribution. The dark areas highlighted by red lines indicate areas of particle incorporation into the coating surface. Quantitatively, the TiO₂+Cr₂O₃ coating showed approximately 25% less mass loss than the TiO₂ coating at 2 m/s, and around 12% less at 4 m/s, confirming its superior erosion resistance. These data highlight the importance of rate

- control during testing to minimize wear loss and provide a more stable coating structure.
- 4. The improved surface properties and wear resistance of TiO₂+Cr₂O₃ coatings emphasize their practical applicability in industrial components exposed to erosive environments, such as pumps, valves, and pipeline systems. These coatings are especially promising for use in mining and hydrometallurgical operations where slag erosion and cavitation are common. Future research will focus on enhancing their performance under such complex service conditions.

Overall, the study showed that the addition of Cr₂O₃ to TiO₂ coatings improves their wear resistance and mechanical stability. An increase in the erosive wear rate leads to the deterioration of the coating structure, which emphasizes the importance of parameter control during testing. The findings open up opportunities for further optimization of coatings in applications where high wear resistance is critical. These findings highlight the technological relevance of thermal spray coatings for erosion-prone environments, offering improved surface hardness and durability. Future studies will focus on optimizing the microstructure of composite coatings and evaluating their performance under cavitation erosion conditions.

Acknowledgment

This research has been funded by the Science Committee of the Ministry of Education and Science of the Republic of Kazakhstan (Grant No. AP19680724).

Gratitude is expressed to Dr Fatih E. Bastan, Leading Researcher of the Thermal Spray Application and Research Laboratory (TESLAB) (Turkey, Sakarya), for his support in conducting analytical analysis and providing valuable recommendations that significantly contributed to the research. We would also like to thank the leadership team and support staff of the Thermal Spray Application and Research Laboratory (TESLAB) for providing infrastructure support for this research.

REFERENCES

 Bastakys, L., Mardare, D., Gherman, A. M. Tribological properties of Cr₂O₃–SiO₂–TiO₂ coatings deposited by atmospheric plasma spraying. Coatings, 2023; 13(2), 408. https://doi.org/10.3390/ coatings13020408

- Bolelli, G., Candeli, A., Lusvarghi, L., Benedetti, L. Hot corrosion behaviour of thermal-sprayed TiO₂-reinforced Cr₂O₃ composite coatings. Journal of Bio- and Tribo-Corrosion, 2021; 7(4), 135. https://doi.org/10.1007/s40735-021-00536-1
- 3. Eraslan, F., Gecü, R., Yılmaz, H. Al₂O₃–TiO₂ hybrid coatings for enhanced wear and corrosion resistance. Materials Today: Proceedings, 2023; 73, 110–118. https://doi.org/10.1016/j.matpr.2023.05.271
- Chen, Y., Liu, F., Zhang, J. Damage evolution of Cr₂O₃–TiO₂ coating under cyclic impact and corrosive environments. Coatings, 2025; 15(1), 98. https://doi.org/10.3390/coatings15010098
- Zhou, X., Li, C., Wang, Q., Sun, X. Ni-Cr-Ti composite coatings for erosion resistance in pump components. Journal of Thermal Spray Technology, 2023; 32(1), 122–134. https://doi.org/10.1007/s11665-023-08041-x
- Goyal, K. Mechanical properties and erosive behaviour of 10 TiO₂+Cr₂O₃ coated turbine steel under accelerated slurry conditions. World Journal of Engineering, 2019; 16(1), 64–70. https://doi.org/10.1108/WJE-08-2018-0262
- Singh, R., Bhatnagar, R. Influence of impact velocity on erosion-corrosion behavior of TiO₂-based thermal spray coatings. Surface Engineering, 2022; 38(5), 483–492. https://doi.org/10.1080/02670844. 2021.1944372
- 8. Finnie I., Erosion of surfaces by solid particles, Wear, 1960; 3, 87–103.
- 9. Finnie I., Some observations on the erosion of ductile metals, Wear, 1972; 19, 81–90.
- 10. Bitter J.G.A., A study of erosion phenomena Part I, Wear, 1963; 6, 5–21.
- 11. Bitter J.G.A., A study of erosion phenomena Part II, Wear, 1963; 6, 169–190.
- 12. Shipway P.H., Hutchings L.M., The role of particle properties in the erosion of brittle materials, Wear, 1996; 193, 105–113.
- 13. Lindsley B.A., Marder A.R., The effect of velocity on the solid particle erosion rate of alloys, Wear, 1999; 225–229, 510–516.
- 14. Barton N.A., Erosion in Elbows in Hydrocarbon Production Systems: Review Document, TÜV NEL Limited, Research Report 115, Glasgow, 2003.
- 15. Adamiak M., Effect of abrasive size on wear, Abrasion Resistance of Materials, InTech, 2012; 167–184.
- 16. Kulu P., Tarbe R., Vallikivi, A., Abrasive wear of powder materials and coatings, Materials Science, 2005; 11, 230–234.
- 17. Lopez D., Congote J.P., Can J.R., Toro A.,

- Tschiptschin A.P., Effect of particle velocity and impact angle on the corrosion–erosion of AISI 304 and AISI 420 stainless steels, Wear, 2005; 259, 118–124.
- 18. Jha A.K., Batham R., Ahmed M., Majumder A.K., Modi O.P., Chaturvedi S., Gupta A. K., Effect of impinging angle and rotating speed on erosion behavior of aluminum, Trans. Nonferrous Met. Soc. China, 2011; 21, 32–38.
- 19. Katsich C., Badisch E., Roy M., Heath G.R., Franek F., Erosive wear of hard faced Fe–Cr–C alloys at elevated temperature, Wear, 2009; 267, 1856–1864.
- Doubek P., Filipek J., Abrasive and erosive wear of technical materials, Acta Univ. Agric. Et Silvic. Mendel. Brun., 2011; 3, 13–22.
- 21. Patil M.S., Deore E.R., Jahagirdar R.S., Patil S.V., Study of the Parameters Affecting Erosion Wear of Ductile Material in Solid-Liquid Mixture, Proc. of the World Congress on Engineering, London, UK, 2011; 2159–2163.
- 22. Franek F., Badisch E., Kirchgassner M., Advanced methods for characterization of abrasion/erosion resistance of wear protection materials, FME Transactions, 2009; 37, 61–70.
- 23. Desale G.R., Gandhi B.K., Jain S.C., Improvement in the design of a pot tester to simulate erosion wear due to solid–liquid mixture, Wear, 2005; 259, 196–202.
- 24. Demirsöz, R., Polat, R., Türk, A., Erdoğan, G. Investigation of the erosive wear behavior of blast furnace granulated slag against steel with and without hard coating. Gazi University Journal of Engineering and Architecture, 2019; 34(1), 103–114. https://doi.org/10.17341/gazimmfd.416467
- 25. Wang, D., Jin, X., Chen, G.Z. Solid state reactions: an electrochemical approach in molten salts. Annu. Reports Sect. C (Phys. Chem.), 2008; 104, 189. https://doi.org/10.1039/b703904m
- 26. Yang, G.-J., Li, C.-J., Han, F., Ohmori, A. Microstructure and photocatalytic performance of high-velocity oxy-fuel sprayed TiO₂ coatings. Thin Solid Films, 2004; 466, 81–85. https://doi.org/10.1016/J. TSF.2004.02.015
- 27. Avcu, E., Fidan, S., Karabay, S., Sınmazçelik, T. Türkiye'de enerji nakil hatlarında kullanılan AA-1070 ile AA-6101 alaşımlarının katı partikül erozyon davranışlarının karşılaştırılması. Journal of the Faculty of Engineering and Architecture of Gazi University, 2012; 27(4), 865–874.
- 28. Avcu, E., Karabay, S. Investigation of Cr₂O₃+TiO₂ coatings on glass-fiber-reinforced composites: adhesion and wear performance. Eurasian Journal of Science and Engineering, 2024; 10(2), 58–66. https://ejons.org/index.php/ejons/article/view/434